

**INVESTIGATIONS OF RESONANTLY  
ENHANCED MULTIPHOTON IONIZATIONS  
OF ATOMIC MERCURY AND POTASSIUM**

By

Kelly Robert Lim Mah

B.Sc., the University of British Columbia, 1982

A THESIS SUBMITTED IN PARTIAL FULFILLMENT OF  
THE REQUIREMENTS FOR THE DEGREE OF  
MASTER OF SCIENCE

in

THE FACULTY OF GRADUATE STUDIES  
DEPARTMENT OF PHYSICS

We accept this thesis as conforming  
to the required standard

THE UNIVERSITY OF BRITISH COLUMBIA

August 1987

© Kelly Robert Lim Mah, 1987

In presenting this thesis in partial fulfilment of the requirements for an advanced degree at the University of British Columbia, I agree that the Library shall make it freely available for reference and study. I further agree that permission for extensive copying of this thesis for scholarly purposes may be granted by the head of my department or by his or her representatives. It is understood that copying or publication of this thesis for financial gain shall not be allowed without my written permission.

Department of Physics

The University of British Columbia  
1956 Main Mall  
Vancouver, Canada  
V6T 1Y3

Date 31 Aug. 1987

## Abstract

Two investigations are reported on the application of resonantly enhanced multiphoton ionization (RMPI) to gaseous mixtures of an atomic vapor and a few Torr of argon. Photon fluxes large enough to ionize atoms by RMPI were produced by focussing down the light from a tunable pulsed dye laser. The irradiances generated were of the order of  $500 \text{ MWcm}^{-2}$ . Ionization was detected by a voltage biased wire electrode that simply collected the photoelectrons either directly or after some gas multiplication. One investigation was the measurement of the dependence of RMPI processes in mercury on the polarization of the incident light for comparisons with theoretical calculations. The processes were four-photon resonant absorptions to either a  $^1S_0$  or  $^1,^3D_2$  level followed by single photon ionization. Complete photoionization of all atoms excited to the resonant levels is established and the measured polarization dependences are found to agree with the calculated polarization dependence for the resonant excitation step of the RMPI process. Unexplained observations of the distortions in the polarization dependence of the ion yield and the absorption linewidth of the  $6d \ ^1D_2$  resonance are discussed. The second investigation was a study of the density dependent electric dipole forbidden two-photon resonant transition  $^2S \rightarrow ^2P$  in three-photon RMPI spectra of the Rydberg states of potassium. Stark interactions are shown to be unlikely and too weak. From the characteristics of the spectra, the excitation process is identified as a laser-assisted collision interaction.

## Table of Contents

Abstract .....	ii
Table of Contents .....	iii
List of Tables .....	iv
List of Figures .....	v
Acknowledgements .....	vi
Chapter 1 Introduction .....	1
1.1 Preliminary remarks .....	1
1.2 Present work .....	4
1.3 Organization of the thesis .....	7
References and notes .....	8
Chapter 2 Polarization dependence of resonant multiphoton ionizations on $^1S_0$ and $^1,^3D_2$ states in atomic mercury .....	10
Chapter 3 Collision-induced forbidden two-photon transitions to atomic Rydberg states of potassium .....	38
Chapter 4 Conclusions .....	50
References and notes .....	53

## List of Tables

Table I. Experimentally fitted polarization dependences for ns $^1S_0$ resonances .....	25
Table II. r.m.s. residuals for the ns $^1S_0$ resonances .....	26
Table III. r.m.s. residuals for the $^{1,3}D_2$ resonances .....	27
Table IV. Experimentally fitted polarization dependences for $^{1,3}D_2$ resonances .....	28

## List of Figures

Fig. 2.1	Polarization dependence of the transition $^1S_0 \xrightarrow{4\hbar\omega} 9s \ ^1S_0 \xrightarrow{\hbar\omega} \text{continuum}$	29
Fig. 2.2	Polarization dependence of the transition $^1S_0 \xrightarrow{4\hbar\omega} 10s \ ^1S_0 \xrightarrow{\hbar\omega} \text{continuum}$	30
Fig. 2.3	Polarization dependence of the transition $^1S_0 \xrightarrow{4\hbar\omega} 6d \ ^1D_2 \xrightarrow{\hbar\omega} \text{continuum and the linewidth (triangles)}$	31
Fig. 2.4	Polarization dependence of the transition $^1S_0 \xrightarrow{4\hbar\omega} 6d \ ^3D_2 \xrightarrow{\hbar\omega} \text{continuum and linewidth (triangles)}$	32
Fig. 2.5	Polarization dependence of the transition $^1S_0 \xrightarrow{4\hbar\omega} 7d \ ^1D_2 \xrightarrow{\hbar\omega} \text{continuum}$	33
Fig. 2.6	Polarization dependence of the transition $^1S_0 \xrightarrow{4\hbar\omega} 7d \ ^3D_2 \xrightarrow{\hbar\omega} \text{continuum}$	34
Fig. 2.7	The shape of the polarization factor $3 + 4\cos 4\beta + \cos 8\beta$	35
Fig. 2.8	The shape of the polarization factor $11 + 8\cos 4\beta - 3\cos 8\beta$	36
Fig. 2.9	The observed linewidth (FWHM) of the $6d \ ^1D_2$ resonance (circles) and the $6d \ ^3D_2$ resonance (squares) as a function of the laser pulse energy	37
Fig. 3.1	Schematic diagram of the photoionization experiment	48
Fig. 3.2	Portion of a potassium resonant multiphoton ionization spectra taken at $T=232^\circ\text{C}$ and with a collection voltage of 10 volts	49

## Acknowledgements

I would like to thank my thesis supervisor, Dr. F. W. Dalby, for the freedom he has given me to explore physics in his laboratory. His support, constant encouragement and patience are gratefully acknowledged. I also thank Dr. A. J. Barnard for reading the manuscript on short notice and for suggesting improvements. To James Booth, Hubert Houtman, Dr. P. Bicchi, Dr. M. H. L. Pryce, and Dr. J. Van der Linde, I am indebted for many valuable discussions. Many thanks to Dr. Grant McIntosh for his assistance on the use of the computing system and for our discussions on plasma physics. The extra efforts and skilful construction of the glass cells by Ernie Williams, and the aid in laser maintenance by Allan Cheuck are gratefully acknowledged. For their assistance on the many experiments, I also thank the summer undergraduate workers: Caren Ahlborn, Cynthia Araujo, Chris Barnard, Julius Chan, and Tat Lee. I wish to dedicate this thesis to my mother, Rosemary Mah, whose support was always there.

## CHAPTER 1

### Introduction

#### 1.1 Preliminary remarks.

A multiphoton transition can be defined as the transition of a quantum system through the near simultaneous absorption of two or more photons. In making the transition, the quantum system has to pass through a succession of intermediate states. Generally the intermediate states are not eigenstates of the quantum system; they are non-stationary states (a superposition of eigenstates) that do not retain energy and are often referred to as *virtual* states. The quantum system can remain in the *virtual* state for a time determined by the uncertainty principal; hence the lifetime of the *virtual* state is approximately the inverse of the amount of energy the *virtual* state is off resonance from the nearest state for which the transition is allowed. Absorption of the next photon must occur while the quantum system is in the *virtual* state. Since its lifetime is very short (usually less than one optical cycle  $\sim 10^{-15}$  sec), the absorption of several photons can be regarded as near simultaneous.

The concept of multiphoton processes was first introduced in 1931 in the theoretical work on simultaneous two-photon absorption by Goeppert-Mayer<sup>1</sup>. However, experimental studies were not feasible until the availability of intense monochromatic sources provided by the invention of high power pulsed lasers. Such light sources are necessary for multiphoton work because of the low transition probability of a multiphoton interaction. The requirement of large light intensity can be

understood from the need that there be a large number of photons present to interact with a *virtual* state during its very short lifetime. The study of multiphoton processes is now a mature field and has been the topic of many reviews<sup>2</sup>.

In photoionization an atom irradiated by electromagnetic radiation is ionized when the energy of an absorbed photon is equal to or larger than the ionization energy of the atom. In multiphoton ionization a bound electron can be liberated from an atom having an ionization energy  $E_i$  with photons of energy  $h\nu$  much less than  $E_i$ . When the sum of the energies of an integral number of the incident photons equals the energy difference between the ground state and an excited bound state of the atom, the ionization process exhibits a resonant enhancement. The field of non-resonant multiphoton ionization is usually studied at very high laser irradiances<sup>3</sup>. Since the off resonance processes are generally at least 100 times less probable than the resonant process in the moderate laser irradiance range ( $10^7$ – $10^9$  W/cm<sup>2</sup>), resonantly enhanced multiphoton ionization (RMPI) is a technique suitable for spectroscopy. In fact, RMPI has become a powerful spectroscopic tool used in the understanding of atomic and molecular structure especially in the exploration of excited and continuum states.

A common and simple RMPI experiment with good sensitivity<sup>4,5</sup> is done by focussing a tunable dye laser beam into a low pressure gas cell. The focussing is necessary to generate the required large photon fluxes. Electrons or ions created by the laser-induced ionization are collected and this signal is recorded as the wavelength of the laser is varied. The spectra will show significant increases in the electron or ion signal where the laser is tuned to resonances; hence the pattern of the excited atomic levels are mapped out.

A RMPI process is usually described as a  $m + n$  photon ionization where  $m$  is the number of photons in the resonant excitation step and  $n$  is the minimum number of photons required to ionize the excited atomic level. When a RMPI process has  $m > 1$ , i.e. a resonant multiphoton transition, excited states which

are very difficult or impossible to access by conventional one photon spectroscopy can be probed with RMPI spectroscopy. Transitions to these levels may be parity forbidden for one photon absorption (electric dipole transition), but may be allowed for a multiphoton transition because of the different selection rules governing multiphoton absorption. Particularly useful is the multiphoton absorption of an even number of photons to access an excited state with the same parity as the ground state. Often, one photon transitions to highly excited states take place in the vacuum ultraviolet (VUV) where convenient light sources or window materials are not available. By using multiphoton absorption, tunable visible lasers can perform essentially as ultraviolet sources for the measurement of absorption spectra in the ultraviolet. Multiphoton techniques have allowed ultraviolet spectroscopy to take advantage of the higher resolutions offered by laser light sources. For example, RMPI has found applications in the investigation of highly excited Rydberg states<sup>6</sup> which have conventional absorption spectra lying in the VUV and require high resolution techniques because of their closely spaced energy levels.

Although the basic measurement of a RMPI experiment is simple to describe, the actual photophysics involved in the RMPI process is quite complex. The non-linear character of the multiphoton interaction and the use of high laser irradiances introduces new physics. Some of the many processes that can be significant in multiphoton interactions are the saturation of resonant transitions and transitions to the continuum<sup>7</sup>, AC Stark shifts and splittings of the resonant state<sup>8,9</sup>, cooperative effects leading to harmonic generation (frequency multiplication), and the competition between RMPI and harmonic generation<sup>10-12</sup>. Modelling an RMPI experiment has been a difficult task because of the many processes that may be significant and must be included in theoretical models. In addition, the experimental parameters are not ideal and not simple to model. For example, the laser sources often have spatial and temporal inhomogeneities, finite bandwidths, and multimode

structure. Comparisons between theory and experiment have been simplified, however, by the many improvements in controlling the parameters of powerful lasers. While there are the new questions and new effects in multiphoton ionization to be explored, the thorough understanding of the present processes of RMPI continues to be a challenge. The further development of theoretical models of broader applicability is required to improve comparisons between theory and experiments with non-ideal behavior. Interest in RMPI continues because: it is a sensitive tool for the exploration of excited states; important in the technology of laser isotope separation, laser-induced fusion, and gas breakdown; and likely to occur whenever strong electromagnetic radiation interacts with matter.

Much of the current experimental development of RMPI spectroscopy has been done with the rarified samples of atomic and molecular beams and supersonic jets with the use of multiple laser beams. However, the application of RMPI spectroscopy to static gaseous samples can still be useful to probe multiphoton dynamics, collective effects, and collision interactions, as the work in this thesis demonstrates.

## 1.2 Present work.

This thesis reports on the RMPI of gaseous mixtures of argon and an atomic vapor (mercury or potassium) at moderate laser irradiances ( $\sim 500 \text{ MW cm}^{-2}$ ). Although both investigations used the same basic experimental techniques, their experimental objectives, as characterized by what experimental parameters were varied, were quite different. In the mercury investigations the most important parameter was the polarization of the incident light. For the studies with potassium, it was the atom concentration.

The mercury investigations involved a  $4 + 1$  ionization process. The initial objective was to extend the previous measurements of the RMPI yield as a function of the incident light polarization by Dalby et al.<sup>13</sup> to the ionizations resonant on  $^1S_0$

and  $1,3D_2$  states. Their methods of calculating the dependence of the RMPI processes on the laser polarization were applied to these resonances. RMPI processes exhibit a polarization dependence because the paths of *virtual* angular momentum states that the multiphoton transition can take is governed by the polarization states of the incident photons (the selection rules are governed by the light polarization). Comparisons of the theoretical polarization dependences to the experimental measurements were to be used to deduce information on the relative photoionization cross sections for the  $1,3D_2$  states. In the course of the work of this thesis the ionization was found to be saturated at these irradiances, i.e. all atoms excited to the resonant state were photoionized. Although the polarization measurements could not be used to extract information on the photoionization cross sections, the experiments were able to demonstrate that the theory was valid in predicting the polarization dependence of the resonant excitation. Some perturbations were observed in the polarization dependence of the RMPI resonant on the  $6d\ 1,3D_2$  states. A polarization dependent linewidth was also observed for these resonances. Possible nonlinearities and perturbations responsible for these effects are suggested.

The  $2 + 1$  RMPI spectra was measured for the  $2S$  and  $2D$  resonances of potassium. This RMPI spectra was first studied by Shen and Curry<sup>14</sup> to measure the Rydberg series of these levels. Atoms in highly excited states are often called Rydberg atoms. When a valence electron of an atom is excited to an orbit of high principal quantum number, the electron is far from the ionic core which is sensed as a point charge. Two aspects of Rydberg atoms must be remembered when they are produced in the conditions of these investigations. The first is that the binding energy of the electron to the ionic core is very small. External electric and magnetic fields can strongly affect the Rydberg atom. The second is the importance of collision interactions with Rydberg atoms because their large geometric size gives them large angular momentum mixing collision cross sections. Perturbations by collisions must be considered even when Rydberg atoms are studied at low pressures.

The RMPI spectrum of potassium vapor was studied as a function of atom density in the range  $\sim 10^{13} \text{ cm}^{-3}$  to  $\sim 4 \times 10^{14} \text{ cm}^{-3}$ . Studies at higher densities were precluded by the rapid deterioration of the glass cells at the temperatures necessary to produce these vapor densities. The interest here was to detect dimer formation at these densities, which are much lower than the densities usually encountered in dimer experiments with heat pipe ovens. In the region of the allowed Rydberg resonances, forbidden two-photon transitions to  $^2P$  states with principal quantum numbers greater than 12 were observed as the density exceeded a threshold of  $\sim 8 \times 10^{13} \text{ cm}^{-3}$ . The object of the potassium investigation presented in this thesis was to determine the cause of the forbidden two-photon transitions. Stark interactions are shown to be very unlikely and the interaction is identified as being similar to the laser assisted collision interactions recently observed by Burkhardt et al.<sup>15</sup> The exact mechanism of the process is not described due to the lack of theoretical work on this new class of collisions. The difficulty of modelling the photon-assisted collision interaction lies in the requirement that the interaction of the photons and the two body collision be simultaneous. The separate processes of either the direct absorption of two photons or short range inelastic collision cannot excite the atom to the Rydberg  $^2P$  states. Several interpretations of the laser assisted collision interaction are currently being investigated, but the common characteristic of these interpretations is the long range nature of the interactions that involve Rydberg atoms. The long range interaction produces a transient but reversible distortion of the atomic states that results in the angular momentum mixing of the Rydberg state. Extremely long range collision interactions between Rydberg alkali atoms and the ground state alkali atoms produce enormous angular momentum mixing cross sections of the order of the Rydberg geometric<sup>16</sup> cross sections. With such large cross sections a collision is likely to occur in the presence of the exciting radiation; that is, the state mixing interaction occurs when a ground state perturber atom is encountered within the Rydberg radius of an atom

undergoing optical excitation. The transition is then actually made on the induced  $d$  component of the final mixed Rydberg state.

Although the study of the forbidden two-photon transitions could be done only over a limited range of experimental parameters, the characteristics of the forbidden transitions are shown to favor the explanation by long range interactions.

### 1.3 Organization of the thesis.

The main body of the thesis is presented in the form of two publication manuscripts. Chapter 2 is the manuscript entitled *Polarization dependence of resonant multiphoton ionizations on  $^1S_0$  and  $^1,^3D_2$  states in atomic mercury* co-authored with F. W. Dalby and C. W. Barnard. Chapter 3 is the manuscript of the letter entitled *Collision-induced forbidden two-photon transitions to atomic Rydberg states of potassium* co-authored with P. Bicchi and F. W. Dalby. The manuscripts have had minor changes made to the table and figure numbering to conform to the graduate theses requirements of the University of British Columbia Library, but the numbering remains consistent within the manuscripts. The referencing style of Chapter 2 remains the same as the manuscript's submitted form.

Since these manuscripts were collaborative efforts, the use of them in the thesis makes the identifications of the original contributions by each author important and necessary. Both investigations were done under the supervision and direction of F. W. Dalby whose criticisms and suggestions taken from our discussions are contained in the manuscripts. In addition, he performed the theoretical calculations for the work of Chapter 2. In the investigations found in Chapter 2, C. W. Barnard collected the data under my supervision and performed some of the data analysis. I performed most of the data analysis, participated in the theoretical calculations, produced the figures and wrote the manuscript. In the investigations of Chapter 3 the experiment and analysis of the data were performed by both P. Bicchi and I. We also shared the writing of the manuscript. Finally, I was responsible for the experimental apparatus and details for both investigations.

Chapter 4 contains the conclusions. Since the manuscripts of Chapters 2 and 3 are self-contained, Chapter 4 contains just a brief summary of the earlier conclusions and some additional remarks on the experiments. Some suggestions for future work are also given.

### References and notes

- <sup>1</sup>M. Goeppert-Mayer, *Ann. Phys.* **9**, 273 (1931).
- <sup>2</sup>the fundamental theoretical work has been reviewed by P. Lambropoulos, *Adv. At. Mol. Phys.* **12**, 87 (1976); examples of current topics can be found in *Multi-photon Ionization of Atoms* edited by S. L. Chin and P. Lambropoulos (Academic Press, Toronto, 1984).
- <sup>3</sup>see, for example, J. Morellec, D. Normand, and G. Petite, *Adv. At. Mol. Phys.* **18**, 97 (1982).
- <sup>4</sup>G. Petty, C. Tai, and F. W. Dalby, *Phys. Rev. Lett.* **34**, 1207 (1975).
- <sup>5</sup>P. M. Johnson, M. R. Berman, and D. Zakheim, *J. Chem. Phys.* **62**, 2500 (1975).
- <sup>6</sup>J. A. C. Gallas, G. Leuchs, H. Walther, and H. Figger, *Adv. At. Mol. Phys.* **20**, 413 (1985).
- <sup>7</sup>S. E. Wheatley, P. Agostini, S. N. Dixit, and M. D. Levenson, *Physica Scripta* **18**, 177 (1978).
- <sup>8</sup>J. S. Bakos, *Phys. Rep.* **31**, 209 (1977).
- <sup>9</sup>M. S. Pindzola, A. H. Glasser, and M. G. Payne, *Phys. Rev. A* **30**, 1800 (1984).
- <sup>10</sup>J. C. Miller, R. N. Compton, M. G. Payne, and W. R. Garrett, *Phys. Rev. Lett.* **45**, 114 (1980).
- <sup>11</sup>M. G. Payne and W. R. Garrett, *Phys. Rev. A* **28**, 3409 (1983).
- <sup>12</sup>G. S. Agarwal and S. P. Tewari, *Phys. Rev. A* **29**, 1922 (1984).
- <sup>13</sup>F. W. Dalby, M. H. L. Pryce, and J. H. Sanders, *Can. J. Phys.* **62**, 419 (1984).
- <sup>14</sup>N. M. Shen and S. M. Curry, *Opt. Commun.* **20**, 392 (1977).

<sup>15</sup>C. E. Burkhardt, M. Ciocca, W. P. Garver, and J. J. Leventhal, Phys. Rev. Lett. **57**, 1562 (1986).

<sup>16</sup>C. E. Burkhardt, R. L. Corey, W. P. Garver, J. J. Leventhal, M. Allegrini, and L. Moi, Phys. Rev. A **34**, 80 (1986).

## CHAPTER 2

### **Polarization dependence of resonant multiphoton ionizations on $^1S_0$ and $^{1,3}D_2$ states in atomic mercury.**

K. R. Mah, F. W. Dalby, and C. W. Barnard.

Physics Department, University of British Columbia, Vancouver, British Columbia, Canada V6T 2A6.

Physics Abstract index: 32.80K Multiphoton processes

## Abstract

The polarization dependences of some resonant multiphoton ionizations in atomic mercury have been measured with a broadband (bandwidth  $\sim 1.5 \text{ cm}^{-1}$ ) multimode dye laser at moderate light intensities ( $\sim 500 \text{ MWcm}^{-2}$ ). The multiphoton processes studied were the absorption of four photons to a resonant  $^1S_0$ ,  $^1D_2$ , or  $^3D_2$  level followed by one photon ionization. Complete saturation of the one photon ionization step results in the ionization of all atoms excited to the resonant level. Because of the saturation of the ionization step, the polarization dependence of the 4-photon excitation to the resonant level is measured. The theory developed by Dalby et al. is shown to give good agreement with the experiment when it is used to calculate the polarization dependence of the multiphoton transition to the resonant level. For the  $6d \ ^1D_2$  resonance, distortions in the polarization dependence and an unusual linewidth dependence on the light polarization were observed. We relate these observations to the AC Stark effect and to the production of the third harmonic of the laser light in the focal volume.

## Introduction

Although the field of resonant multiphoton ionization has made much progress over the past decade there are still relevant questions which have not been resolved experimentally. A knowledge of photoionization cross sections from excited states is of interest in testing quantum mechanical calculations and in astrophysical applications, yet the accurate determination of such cross sections is still a challenge. Smith et al. (1) have measured absolute ionization cross sections of the 5S and 4D states of sodium to about 10% accuracy. Their experimental technique used step-wise excitation to the excited state followed by saturating the transition into the continuum, and required three lasers. Angular distributions of photoelectrons produced by multiphoton ionization via an excited resonant state  $l$  are sensitive to the relative cross sections for  $l \rightarrow l + 1$  and  $l \rightarrow l - 1$ . Such work has been reviewed recently by Leuchs and Walther (2). Dalby et al. (3) have studied resonant multiphoton ionization in mercury as a function of the polarization of the exciting laser light. Their theoretical calculations have shown the dependence of the total ionization on the light polarization to be sensitive to certain relative photoionization cross sections. Measurement of the total ionization as a function of the light polarization may yield interesting information and is considerably easier to perform than the saturation method of Smith et al. or the study of photoelectron angular distributions.

We present here the calculated and measured polarization dependences for 5-photon ionizations resonant on  $^1S_0$  and  $^1,^3D_2$  levels in atomic mercury. Our original objective was to determine relative photoionization cross sections for the  $^1,^3D_2$  levels using the technique suggested by Dalby et al. A re-examination of the experimental conditions of the previous work by Dalby et al. suggests that their work was unjustified in the neglect of nonlinear effects in the absorption processes. We have found that the experiments are strongly affected by saturation behavior and the broadening effects associated with a multimode laser; the technique therefore,

is severely limited for producing accurate relative photoionization cross sections. However, careful analysis of our results shows the method used to calculate the polarization dependences is able to predict successfully the experimental dependences.

## Experimental

Light from a Molelectron nitrogen pumped dye laser is focussed with an 82 mm focal length lens into a pyrex proportional counter containing 20 Torr of argon and mercury vapour. The mercury density is temperature controlled with the temperature ranging from 170 K, giving a mercury partial pressure of 6 Torr, to 210 K, giving a partial pressure of 25 Torr. The primary photoelectrons after proportional amplification produce signals which are amplified, processed with a Princeton Applied Research boxcar integrator, and displayed on a strip recorder. The voltage applied to the proportional counter ranged from 400 volts to 670 volts and produced an amplification factor from 10 to 20 and a static electric field at the beam focus from 220 volts/cm to 350 volts/cm.

The 5 ns laser pulse had energies ranging from 100  $\mu\text{J}$  to 350  $\mu\text{J}$ . The boxcar integrator performed averaging over 10 laser pulses. In the focal region the peak ionization probability per pulse is less than  $10^{-5}$  so that the atoms in the focal volume were far from being completely ionized.

A high quality prism polarizer external to the laser cavity ensures that the laser light is linearly polarized to better than one part in  $10^5$ . The light then passes through a Soleil-Babinet compensator accurately tuned as a quarter wave plate. The compensator angle  $\beta$  determines the polarization state of the light with the light being plane polarized for  $\beta = 0^\circ$ , circularly polarized for  $\beta = 45^\circ$  and elliptically polarized otherwise.

After the laser is tuned to the peak of a resonance, the photoelectron signal is measured as a function of the compensator angle  $\beta$ . The experimentally determined

photoionization signals plotted against  $\beta$  are presented for several resonances in Figs. 2.1 to 2.6.

The process  ${}^1S_0 \xrightarrow{4\hbar\omega} n{}^1S_0 \xrightarrow{\hbar\omega} P$  continuum

All transitions studied originate from the  $6s {}^1S_0$  ground state of mercury. The work in reference (3) has shown that the intensity  $I$  of the photoionization signal can be expressed in the form

$$[1] \quad I(\beta) = a_0 + a_1 \cos 4\beta + a_2 \cos 8\beta + \dots$$

For the 5-photon processes studied here, three terms in the Fourier series [1] were sufficient according to the theory. The photionization signal produced by the resonant absorption of four photons to an excited  ${}^1S_0$  level followed by single photon ionization is predicted by reference (3) to be

$$[2] \quad I_s = C_s(3 + 4\cos 4\beta + \cos 8\beta)$$

where  $C_s$  is a constant independent of the polarization state of the laser light. This result, calculated for electric dipole transitions, contains only one adjustable parameter, the scale height  $C_s$ . Moreover, for this case, the transition to the excited  ${}^1S_0$  level without subsequent photoionization has the same polarization dependence [2]. Because both processes have the same polarization dependence and saturation of the ionization of the resonant level is quite possible, the study of such resonances provides a good test of the experimental technique, particularly in testing the linearity of the overall detecting system. If the ionization of the resonant level is saturated, i.e., all atoms which reach the resonant level are ionized, the polarization dependence of the transition to the excited  ${}^1S_0$  level would be observed.

The experimentally determined polarization dependences are obtained by Fourier analyzing the measured polarization dependences to determine the coefficients in eqn. [1]. The experimental polarization dependences for the 9s  $^1S_0$  and 10s  $^1S_0$  resonances are listed in Table I and the root mean square (r.m.s.) residuals in Table II. The Fourier fits have been normalized to a peak of 8 units in order to make direct comparisons with the theoretical prediction [2]. In Table II the r.m.s. residuals are based on the scaling used in the figures. The residual of a data point is the difference between the value derived from the Fourier fitted curve (or the theoretical curve) and the experimental value. The experimental points, the fitted Fourier curve (solid curves), and the theoretical curve predicted by eqn. [2] (broken curves) are shown in Fig. 2.1 for the 9s  $^1S_0$  resonance, and in Fig. 2.2 for the 10s  $^1S_0$ . The peak signal intensities in the figures have been normalized to 100 units and the experimental accuracy for a single observation is better than  $\pm 5$  units. The displayed theoretical curves have their scale height adjusted to fit the data. Both curves fit the data reasonably well and the r.m.s. residuals, which are a measure of the goodness of the fit, are within the experimental uncertainty.

We conclude from the rather good agreement between the observations and the theory for the  $^1S_0$  resonances that the proportional counter and the amplifying system are reasonably linear and do not significantly modify the shape of the plots of the photoionization signal as a function of compensator angle.

The process  $^1S_0 \xrightarrow{4h\nu} n^{1,3}D_2 \xrightarrow{h\nu} \text{continua}$

Excited D states can be photoionized into a P continuum with a cross section  $\sigma_{d \rightarrow p}$  and into a F continuum with a cross section  $\sigma_{d \rightarrow f}$ . From reference (3) we calculate the total multiphoton ionization signal intensity,  $I_d$  for the 4 + 1 photon process resonant on  $^1D_2$  and  $^3D_2$  levels to be

$$[3] \quad I_d = C_d [28(3 + 4\cos 4\beta + \cos 8\beta)\sigma_{d \rightarrow p} + 9(11 + 8\cos 4\beta - 3\cos 8\beta)\sigma_{d \rightarrow f}]$$

where  $C_d$  is a constant independent of the polarization of the of the exciting laser light. The theoretically calculated shape for ionization into the P continuum is proportional to  $3 + 4\cos 4\beta + \cos 8\beta$  and is displayed in Fig. 2.7 For ionization into the F continuum the shape is proportional to  $11 + 8\cos\beta - 3\cos 8\beta$  and is displayed in Fig. 2.8 The measured polarization dependence for the  $1,3D_2$  resonances should be a linear superposition of these two curves. By comparing the observed ionization dependence on polarization with that predicted theoretically by eqn. [3] we originally planned to deduce relative values of the cross sections i.e.,  $\sigma_{d \rightarrow p} / \sigma_{d \rightarrow f}$ . As we explain later, the nonlinear processes present in our experiments make eqn. [3] invalid in describing the data.

Our observations of the photoionization signals resonant on the  $6d \ ^1D_2$ ,  $6d \ ^3D_2$ ,  $7d \ ^1D_2$ ,  $7d \ ^3D_2$  levels are shown in Figs. 2.3 to 2.6. Again the experimental accuracy for a single observation is  $\pm 5$  units. The solid curves are the Fourier fits to the data. The r.m.s. residuals between the experimental measurements and the Fourier fits are tabulated in Table III.

## Discussion

We have carefully performed the straightforward measurement of the photoionization yield as a function of laser polarization. The theoretical expressions used to fit the data and from which relative cross sections for the excited states could be deduced are applicable in the limit of vanishing laser intensity, and in the absence of significant interactions between the atoms. However, in order to perform these measurements with an adequate signal to noise ratio, moderate laser irradiances are necessary. In addition, the atomic densities required to get adequate signal levels could be large enough to make the assumption that the atoms are non-interacting incorrect. How well the lowest order theory used here is applicable to the experimental conditions and what are the effects of saturation are questions that arise. It is difficult to derive the theory which accurately takes into account

saturation behavior for the rather wide laser bandwidths ( $\sim 1.5 \text{ cm}^{-1}$  in our work) commonly used in multiphoton ionization experiments. At present we are not aware of such a theory and we attempt to address these questions experimentally.

### AC Stark Effect

In addition to saturation behavior, we believe that some of the polarization measurements were perturbed by the AC Stark effect. The lowest order theory from reference (3) does not take into account this effect. In the measurement of the polarization dependence of the  $6d \ ^1D_2$  resonance, we observed several features that were not observed for the other resonances. We remark that the spectral lineshape of the  $6d \ ^1D_2$  resonance exhibits an asymmetric broadening and lineshift to the red with increasing laser irradiances. In Fig. 2.9 the observed linewidth (the full width at half maximum) as a function of the laser pulse energy is presented for the  $6d \ ^1D_2$  and  $6d \ ^3D_2$  resonances. For all the transitions studied except the  $6d \ ^1D_2$  resonance, the slope of the linewidth vs. pulse energy plots are essentially equal to the slope exhibited by the plot for the  $6d \ ^3D_2$  resonance. The linewidth of the  $6d \ ^1D_2$  resonance is considerably more sensitive to the laser power density. Reif et al. (4), (5) have observed and explained the asymmetric spectral lineshape and the large lineshift of the  $6d \ ^1D_2$  resonance as a result of the AC Stark coupling of the  $6d \ ^1D_2$  level to the  $6d \ ^1P_1$  level. These effects are power-dependent and with large irradiances (on the order of  $100 \text{ GWcm}^{-2}$ ), Reif et al. observed large effects. Even though our polarization measurements were performed at relatively low laser irradiances (a pulse energy of  $250 \ \mu\text{J}$  corresponds to a power flux of  $\sim 600 \text{ MWcm}^{-2}$ ), the asymmetry and broadening of the spectral line were noticeable.

Another feature observed only for the  $6d \ ^1D_2$  resonance was that its linewidth varied with the light polarization as displayed in Fig. 2.3. None of the other resonances studied displayed such an effect. The absence of the linewidth dependence for the other resonances is demonstrated in Fig. 2.4 for the  $6d \ ^3D_2$  resonance. We

believe the laser-induced coupling of the  $6d\ ^1D_2$  level to the  $6d\ ^1P_1$  level is responsible for the polarization dependence of the linewidth, but we cannot provide a theory of the mechanism. Since the peak signal intensities are affected by the variation of linewidth with polarization, the polarization curve becomes distorted. The distortion could be a reason the theoretical curve in Fig. 2.3 fits the data less well than the theoretical curve in Fig. 2.4. The appropriate theoretical curve for these measurements will be explained later in the section on saturation behavior.

### Frequency Tripled Light

Another nonlinearity not included in the lowest order theory is the production of light at triple the laser frequency. This effect might be unexpected for a 4-photon resonant transition. However, at mercury pressures above  $5 \times 10^{-2}$  Torr and with a 350 mm focal length lens and laser irradiances over a factor of 100 greater than ours, Normand et al. (6) have observed strong vacuum ultraviolet (VUV) emission at three times the laser frequency near the 4-photon resonances of the  $6d\ ^1D_2$  level and more weakly, the  $6d\ ^3D_2$  level and the effects of the VUV light on the resonant multiphoton ionization signals. At considerably higher pressures (above 20 Torr), we have observed similar effects which we believe to be due to the production of VUV light although we do not measure the VUV light directly. We observe that these effects are strongly dependent on mercury pressure. At the mercury densities used here the cooperative effects which lead to significant frequency tripling are negligible for the  $7d\ ^1,^3D_2$  resonances. The production of VUV light can affect the polarization measurements because the reabsorption of the VUV photon followed by the absorption of two laser photons also produces a resonant ionization signal. Since this three-photon ionization process has a different polarization dependence from the 5-photon process, the signal component involving the VUV photon contaminates the polarization curves. The possibility that the polarization curves are somewhat distorted for the  $6d\ ^1,^3D_2$  resonances by frequency tripling, AC Stark effect, and

polarization dependent linewidths is reflected in the relatively large residuals for their Fourier fitted curves as shown in Table III.

### Saturation Behavior

Two types of saturation processes in the multiphoton absorptions need to be considered. Saturation of the transition to the resonant level occurs when the ground state is significantly depopulated. Because the excitation step in our studies requires four photons, saturation occurs only at much larger laser irradiances than those used here. Under our experimental conditions, we estimate the multiphoton probability of populating the resonant level  $7d\ ^1D_2$  to be  $\sim 10^{-7}$  (the tables of Bates and Damgaard (7) were used in the evaluation of the appropriate matrix elements); therefore, the ground state is not significantly depopulated and saturation of the excitation process can be ignored. Also possible is the saturation of the ionization step which must be considered when the ionization rate is greater than the rate of relaxation of the resonant level. Provided that the excitation rate is extremely low, the result of this type of saturation is the ionization of all the excited atoms. This type of saturation causes the absorption process to have the polarization dependence of the 4-photon transition to the resonant level since all atoms excited to the resonant level are taken into the continuum independent of the polarization of the light.

Over the range of irradiances studied, we found the signals for the 5-photon ionizations to be proportional to the third power of the laser irradiance. By examining how the ionization probability depends on the irradiance, information about the extent of the saturation of the ionization step can be deduced. For this discussion we use a resonant multiphoton ionization probability which omits details concerning the laser bandwidth, mode structure, and the spatial inhomogeneities of the laser intensity in the interaction region. While these experimental aspects have been neglected in order to simplify the analysis, this ionization probability

possesses the necessary features to describe qualitatively the observed power dependence. The ionization probability does contain the mechanisms of the distortion of the atomic structure in the light field, i.e., the shift and broadening of the atomic level. The broadening of the resonant level is a dominant experimental feature even though the laser linewidth is already much greater than the natural linewidth. The observed resonance linewidth is even greater than the laser linewidth and it has a linear dependence on the light intensity as displayed in Fig. 2.9. Assuming there is no saturation of the 4-photon excitation step, the ionization probability for a 4-photon resonant absorption followed by one photon ionization is (8)

$$[4] \quad W = \beta^{(5)} \frac{I_l^5}{(E_s^{(0)} - E_g^{(0)} + c'_s I_l - 4E_p)^2 + (\gamma^{(0)} + d'_s I_l)^2}$$

where  $\beta^{(5)}$  is the generalized cross section of the process and does not depend on the light intensity,  $I_l$ .  $E_s^{(0)}$  and  $E_g^{(0)}$  are the energies of the unperturbed resonant and initial level, respectively.  $E_p$  is the photon energy and  $\gamma_s$  is the natural width of the resonant level  $s$ . Finally, the Stark constant,  $c'_s$  is  $c_s - c_g$  where  $c_s$  and  $c_g$  are the Stark constants of the resonant level and the initial level, respectively and  $d'_s$  is  $d_s - d_g$  where  $d_i$  is the coefficient of induced-broadening. The term describing the width of the resonant level,  $\gamma_s + d'_s I_l$ , is the inverse of the lifetime of the resonant level. For large light intensities such that  $d'_s I_l \gg \gamma_s$ , the lifetime of the resonant level is reduced significantly by the photoionization. When this occurs, most atoms excited to the resonant level are ionized; thus, the ionization step is saturated. Under the conditions for saturation, the linewidth term becomes effectively proportional to  $I_l$  and the ionization probability at resonance displays the observed cubic power dependence. Using the formula of Burgess and Seaton (9) we estimate the photoionization cross section for the 7d  $^1D_2$  resonance to be  $2 \times 10^{-18} \text{ cm}^2$  and the photoionization rate with our irradiances to be greater than

$2 \times 10^9 \text{ s}^{-1}$ . With the natural lifetime of the  $7d \ ^1D_2$  level being 40 ns (10) and interaction lasting 5 ns saturation of the ionization step is realized.

The observed line broadening is due to the inhomogeneous line broadening by the Stark shift  $c'_s I_l$  and not due to the shortening of the resonant level lifetime by the large ionization rate.

A theory sophisticated enough to give the polarization dependence when there is partial saturation of the ionization step is not yet available. For ionization processes with partial saturation, we would not be able to explain quantitatively the observed polarization dependences. However, since the ionization step was completely saturated, the data can be fitted to the polarization dependence of the 4-photon excitation process. For excitation to the  $^1,^3D_2$  levels the calculated dependence is according to reference (3)

$$[5] \quad I = C_d(9 + 8\cos 4\beta - \cos 8\beta)$$

where  $C_d$  is a constant independent of the polarization of the light. This theoretical form was fitted to the data and is shown along with the Fourier fits in Figs. 2.3 to 2.6. The r.m.s. residuals for this curve are given in Table III. The Fourier fits, which are normalized to 16 units to facilitate comparisons with the theoretical form [5], are tabulated in Table IV. The theoretical curves fit the data adequately and, within the sensitivity of the experiment, the Fourier curves show good agreement with the theoretical curves. Further evidence of the validity of the theory is provided by the excellent agreement the theoretical curves have with the data of the  $^1S_0$  resonant ionizations.

Complete saturation of the ionization step makes it impossible to extract relative photoionization cross sections from the data with eqn. [3]. Saturation behavior limits the usefulness of the experiment for this purpose and we are unable to characterize quantitatively the effect of this nonlinearity. How the polarization

dependence behaves under conditions of partial saturation is an investigation we cannot perform because our present detection system lacks the sensitivity to do studies at much lower irradiances. However we have found the other nonlinear effects present in the experiment produce noticeable distortions in the data as in the case of the  $6d\ ^{1,3}D_2$  resonances which were affected by the AC Stark effect and possibly frequency tripling.

### Collisional Effects

Collisions that lead to ionization of the resonant level or to changes in the angular momentum of the resonant level will cause the observed polarization dependence to differ from the calculated dependence. Saturation of the ionization step makes the transition into the continuum almost independent of the light polarization. Because of the saturation of the ionization step, we measure just the polarization dependence of the excitation step. The collisions described above have almost no effect on our experiment because they affect the multiphoton process after the resonant level has been populated.

### Conclusions

In reference (3) Dalby et al. developed a theory for the polarization dependences of resonant multiphoton ionization processes and used it to fit polarization data for 3 and 4-photon resonances with subsequent one photon ionization. Although their neglect of saturation effects makes the above application invalid, we have shown that their theory gives good agreement with experiment when it is used to calculate the polarization dependence of the multiphoton transition to the resonant level. The measurement of polarization dependences is severely limited for the determination of relative photoionization cross sections for the 4-photon resonant absorptions with subsequent one photon ionization because of the great difference

in the magnitude of the transition probabilities of the excitation step and the ionization step. The stronger coupling to the continuum makes the experiment very difficult to perform without saturating the ionization step.

The new observations of the polarization dependent linewidths and the modifications of the polarization dependence when there is AC Stark coupling of intermediate levels with the resonant level will require more theoretical work.

### **Acknowledgements**

We are grateful for the help with the collection and analysis of data by Caren Ahlborn and Tat Lee. We thank James Booth, Maurice Pryce, and Luis de Sobrino for helpful suggestions and critical reading of the manuscript. This work was supported by the Natural Sciences and Engineering Research Council of Canada.

## References

1. A. V. Smith, J. E. M. Goldsmith, D. E. Nitz and S. J. Smith. *Phys. Rev. A*, **22**, 577 (1980).
2. G. Leuchs and H. Walther, in *Multiphoton Ionization of Atoms*. edited by S. L. Chin and P. Lambropoulos. Academic Press, New York, 1984.
3. F. W. Dalby, M. H. L. Pryce, and J. H. Sanders. *Can. J. Phys.* **62**, 419 (1984).
4. J. Reif, M. Poirier, J. Morellec, and D. Normand. *J. Phys. B*, **17**, 4151 (1984).
5. J. Reif, J. Morellec, D. Normand and M. Poirier. presented at 2nd European Conference on Atomic and Molecular Physics, Amsterdam, April 15-19, 1985. Paper WE85.
6. D. Normand, J. Morellec and J. Reif. *J. Phys. B*, **17**, L227 (1983).
7. D. R. Bates and A. Damgaard. *Philos. Trans. R. Soc. London, Ser. A*, **242**, 101 (1949).
8. J. S. Bakos. *Phys. Reports* **31**, 209 (1977).
9. A. Burgess and M. J. Seaton. *Rev. Mod. Phys.* **30**, 992 (1958).
10. A. A. Radig and B. M. Smirnov, *Reference Data on Atoms, Molecules, and Ions*. Springer-Verlag, Berlin, 1985. p. 246

Table I. Experimentally fitted polarization dependences for  $ns\ ^1S_0$  resonances.

n	Polarization dependent factor
9	$(3.12 \pm 0.06) + (4.01 \pm 0.09)\cos 4\beta + (0.87 \pm 0.09)\cos 8\beta$
10	$(3.27 \pm 0.05) + (4.07 \pm 0.08)\cos 4\beta + (0.66 \pm 0.08)\cos 8\beta$

Table II. r.m.s. residuals for the  $ns \ ^1S_0$  resonances.

n	$\langle (I_{\text{experimental}} - I_{\text{Fourier}})^2 \rangle^{1/2}$	$\langle (I_{\text{experimental}} - I_{\text{theoretical}})^2 \rangle^{1/2}$
9	4.6	4.8
10	2.3	4.6

Table III. r.m.s. residuals for the  $1,3D_2$  resonances.

resonance	$\langle (I_{\text{experimental}} - I_{\text{Fourier}})^2 \rangle^{1/2}$	$\langle (I_{\text{experimental}} - I_{\text{theoretical}})^2 \rangle^{1/2}$
6d $1D_2$	4.4	5.2
6d $3D_2$	4.6	5.5
7d $1D_2$	2.5	3.9
7d $3D_2$	2.9	4.8

Table IV. Experimentally fitted polarization dependences for  $1,3D_2$  resonances.

resonance	polarization dependent factor
6d $1D_2$	$(8.64 \pm 0.18) + (7.72 \pm 0.26) \cos 4\beta - (0.36 \pm 0.26) \cos 8\beta$
6d $3D_2$	$(9.56 \pm 0.19) + (7.94 \pm 0.27) \cos 4\beta - (1.50 \pm 0.27) \cos 8\beta$
7d $1D_2$	$(8.46 \pm 0.10) + (7.94 \pm 0.15) \cos 4\beta - (0.39 \pm 0.15) \cos 8\beta$
7d $3D_2$	$(8.26 \pm 0.12) + (8.08 \pm 0.17) \cos 4\beta - (0.35 \pm 0.17) \cos 8\beta$

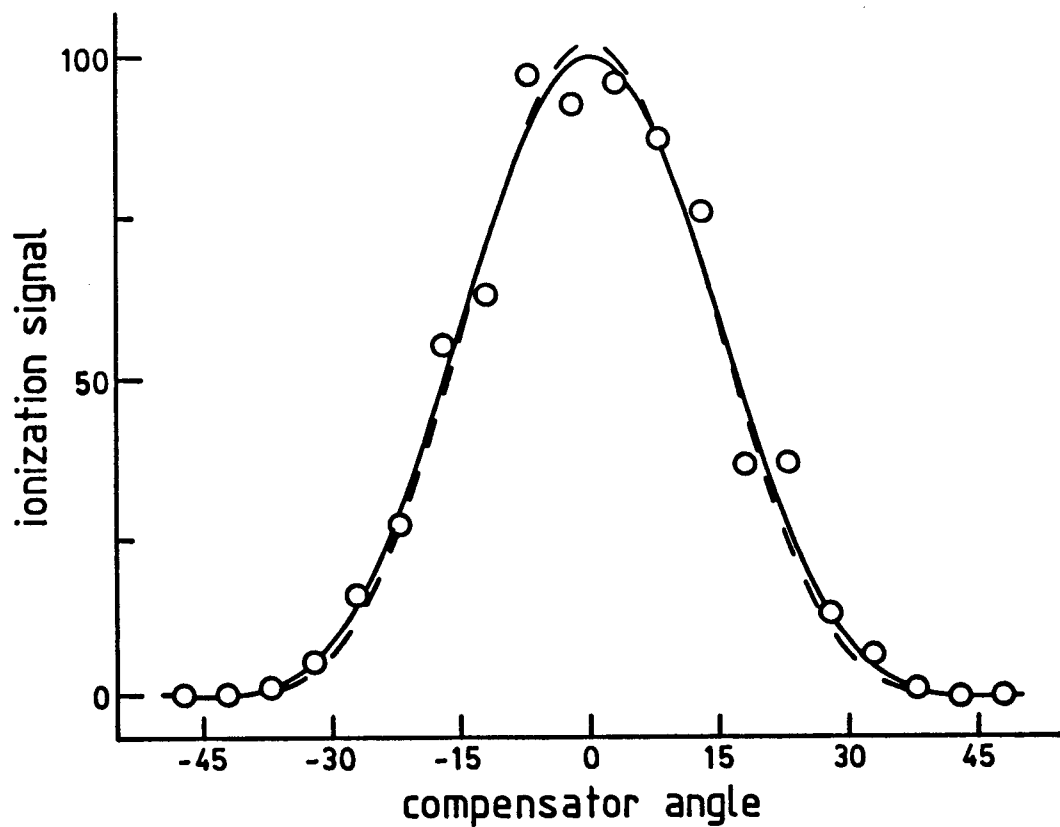


Fig. 2.1 Polarization dependence of the transition  $1S_0 \xrightarrow{4\hbar\omega} 9s\ 1S_0 \xrightarrow{\hbar\omega} \text{continuum}$  as a function of the compensator angle  $\beta$ . At  $\beta = 0^\circ$  the incident light is linearly polarized and  $\beta = \pm 45^\circ$  corresponds to circularly polarized light. The solid curve is the Fourier fit of form [1] and the peak of the curve is normalized to 100 units. The broken curve is the theoretical curve given by eqn. [2]

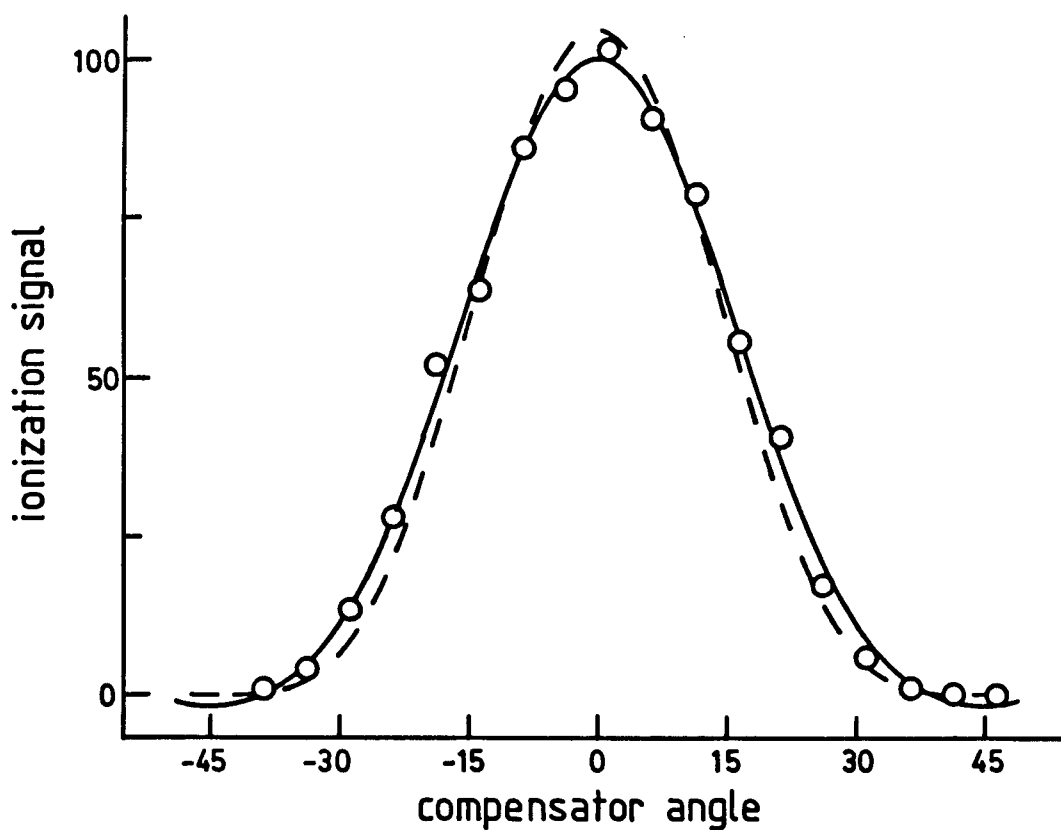


Fig. 2.2 Polarization dependence of the transition  ${}^1S_0 \xrightarrow{4\hbar\omega} 10s\ {}^1S_0 \xrightarrow{\hbar\omega} \text{continuum}$  as a function of the compensator angle. The solid curve is the Fourier fit to the ionization data and the broken curve is the theoretical curve given by eqn. [2].

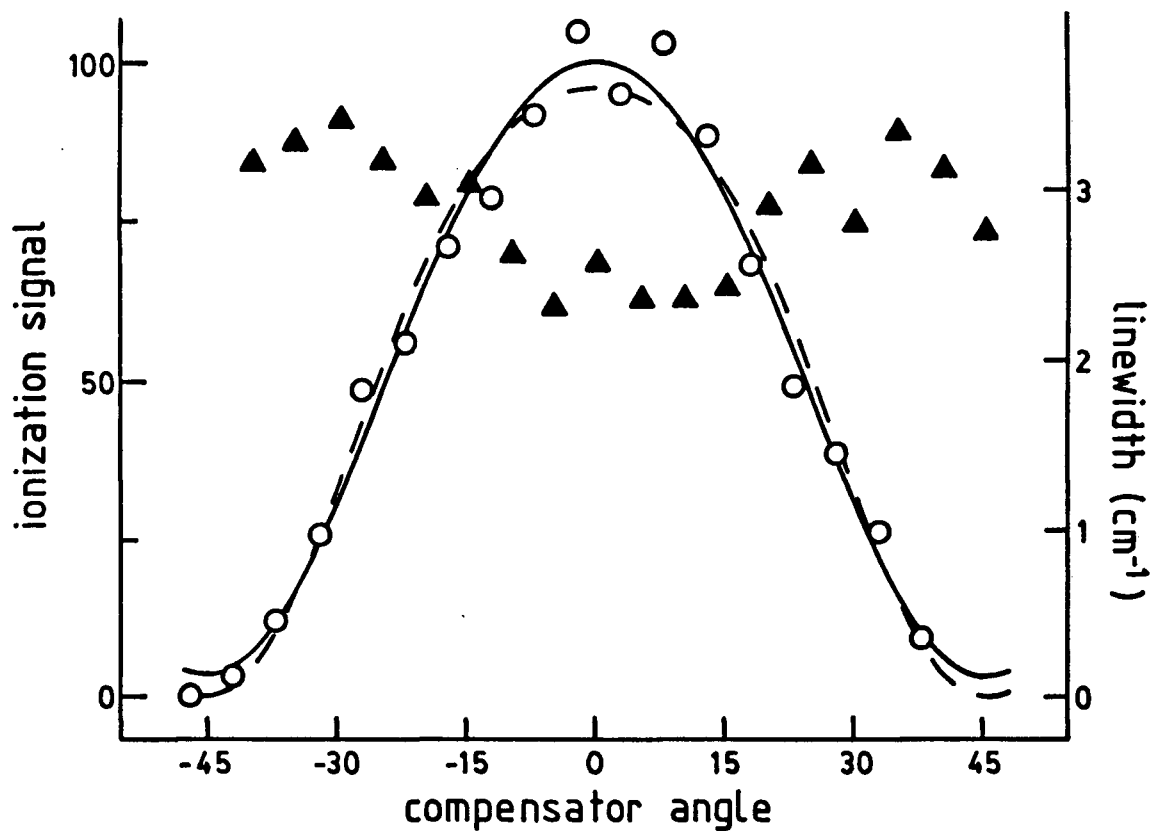


Fig. 2.3 Polarization dependence of the transition  $1S_0 \xrightarrow{4\hbar\omega} 6d\ 1D_2 \xrightarrow{\hbar\omega} \text{continuum}$  and the linewidth (triangles) as a function of the compensator angle. The solid curve is the Fourier fit to the ionization data and the broken curve is the theoretical curve given by eqn. [5]. The linewidth exhibits a variation with the compensator angle.

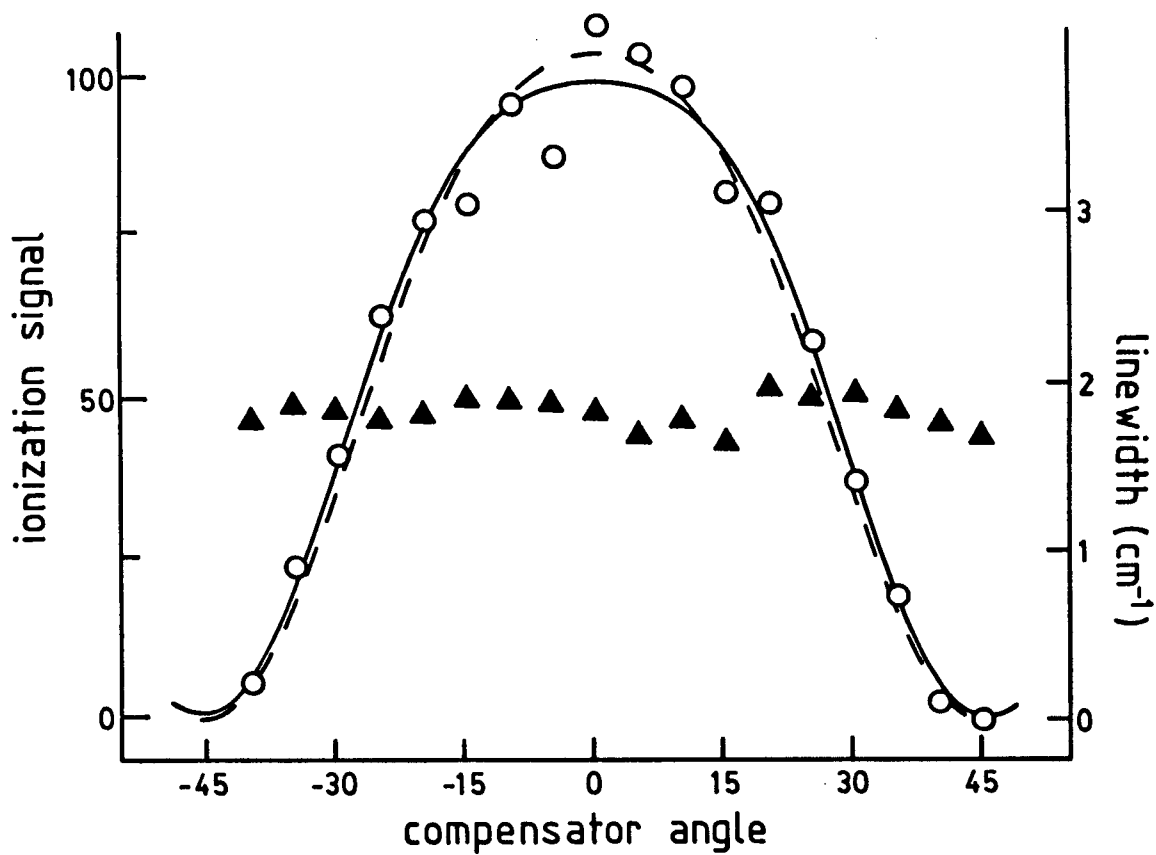


Fig. 2.4 Polarization dependence of the transition  ${}^1S_0 \xrightarrow{4\hbar\omega} 6d\ {}^3D_2 \xrightarrow{\hbar\omega} \text{continuum}$  and the linewidth (triangles) as a function of the compensator angle. The solid curve is the Fourier fit to the ionization data and the broken curve is theoretical curve given by eqn. [5].

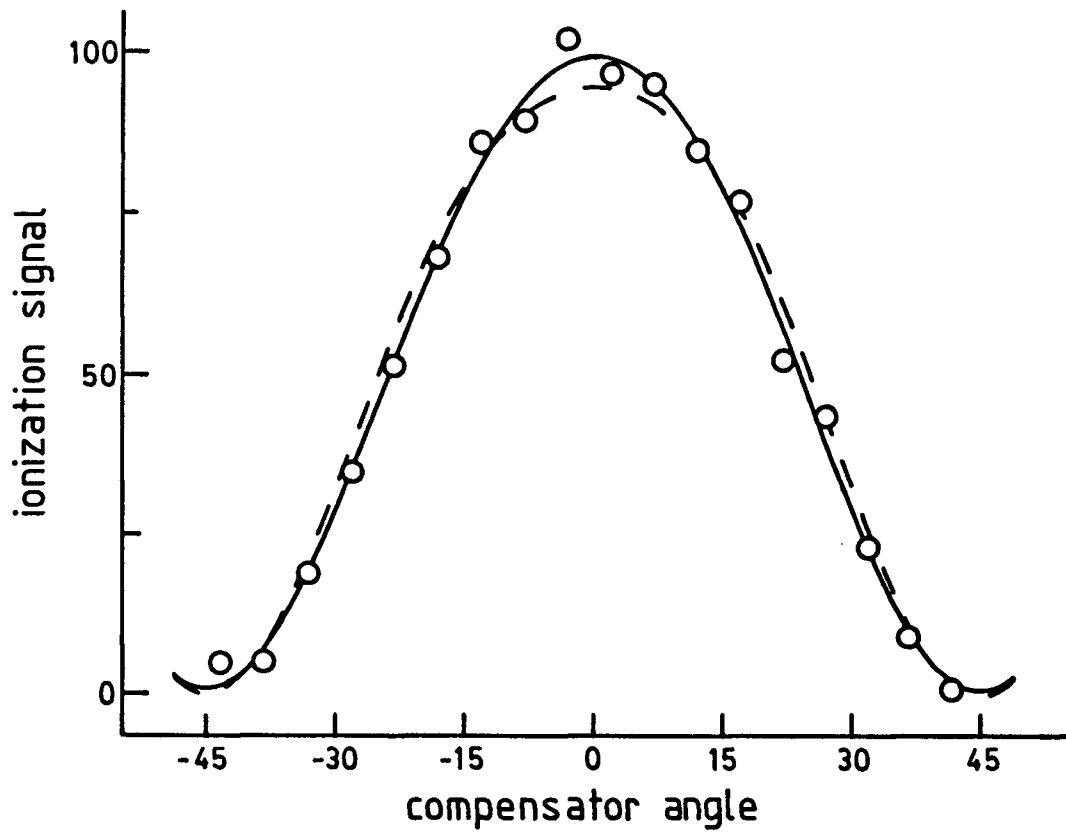


Fig. 2.5 Polarization dependence of the transition  $1S_0 \xrightarrow{4\hbar\omega} 7d \ 1D_2 \xrightarrow{\hbar\omega} \text{continuum}$  as a function of the compensator angle. The solid curve is the Fourier fit to the ionization data and the broken curve is the theoretical curve given by eqn. [5].

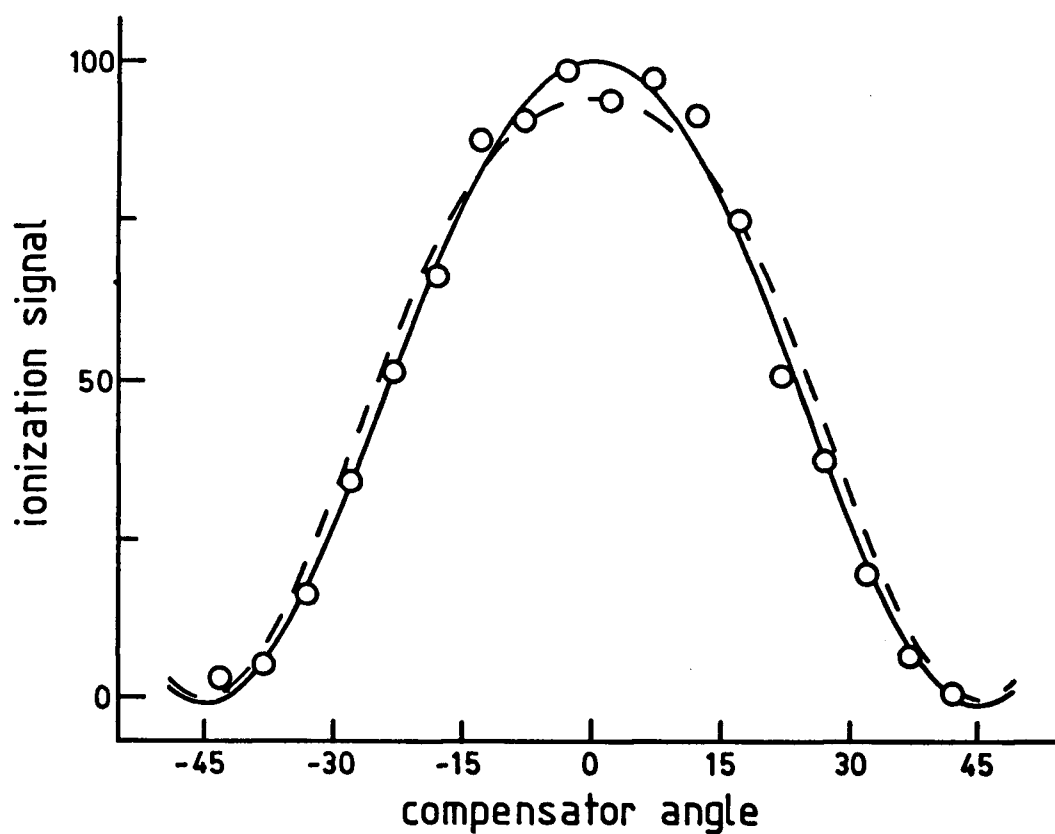


Fig. 2.6 Polarization dependence of the transition  $^1S_0 \xrightarrow{4\hbar\omega} 7d \ ^3D_2 \xrightarrow{\hbar\omega} \text{continuum}$  as a function of the compensator angle. The solid curve is the Fourier fit to the ionization data and the broken curve is the theoretical curve given by eqn. [5].

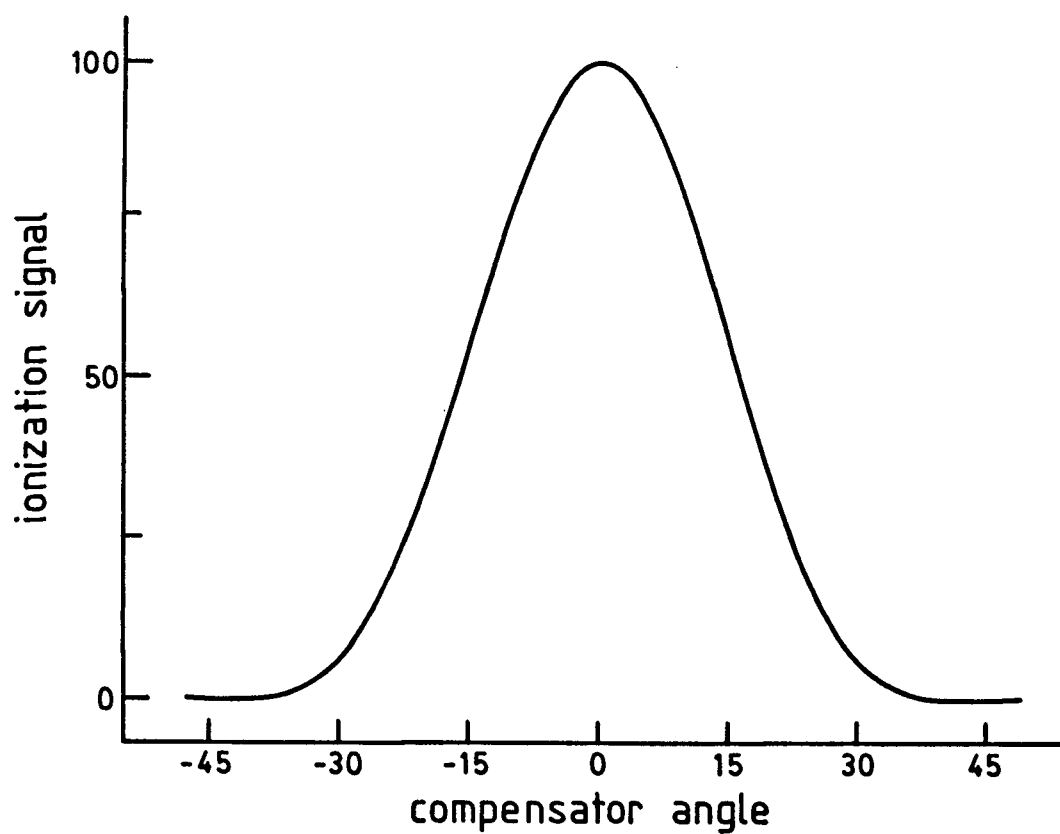


Fig. 2.7 The shape of the polarization factor  $3 + 4\cos 4\beta + \cos 8\beta$ . This is the polarization dependence of 4-photon resonant transitions with subsequent single photon ionization into a P continuum.

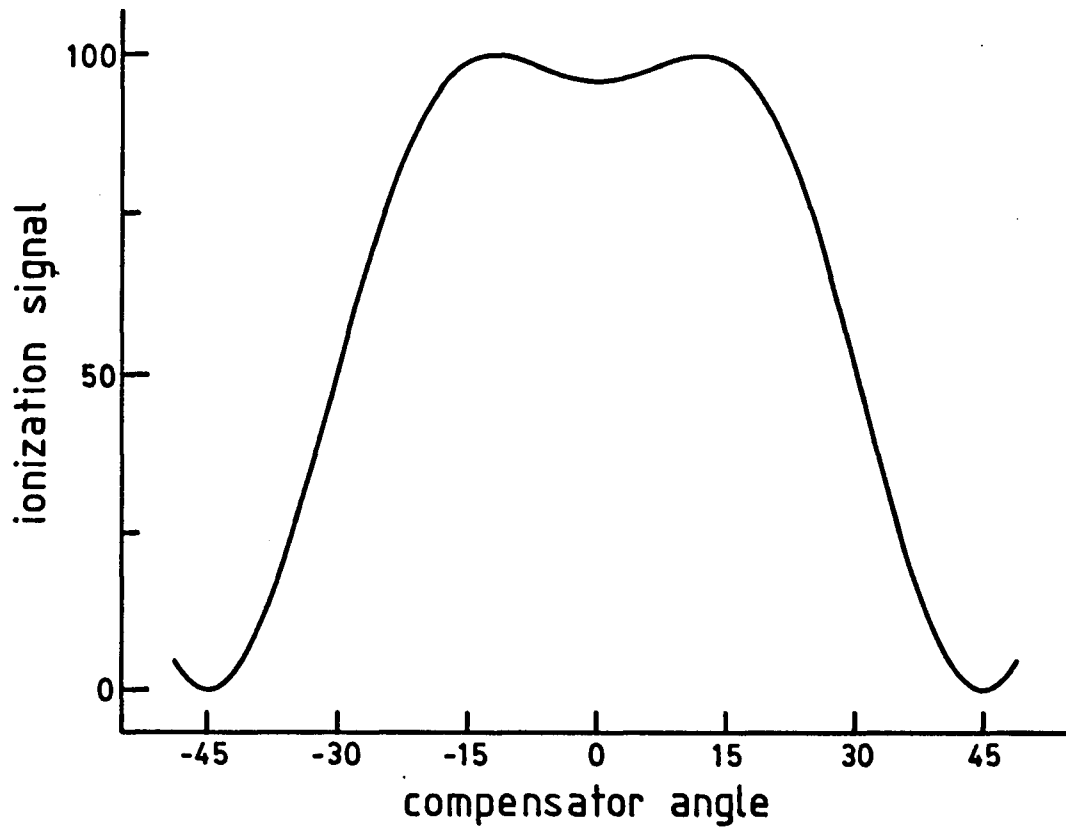


Fig. 2.8 The shape of the polarization factor  $11 + 8\cos 4\beta - 3\cos 8\beta$ . This is the polarization dependence of 4-photon resonant transitions with subsequent single photon ionization into a F continuum.

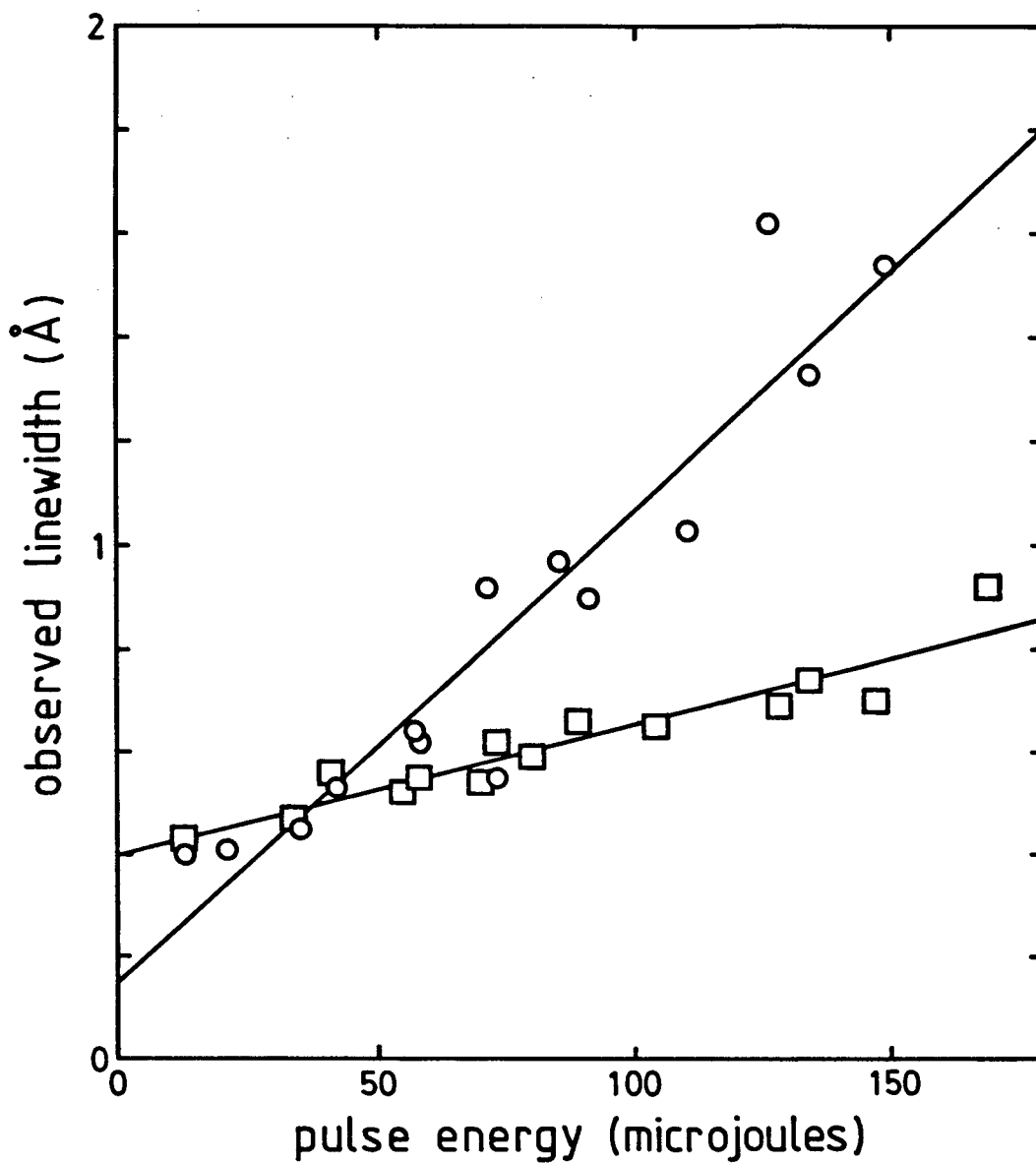


Fig. 2.9 The observed linewidth (FWHM) of the 6d <sup>1</sup>D<sub>2</sub> resonance (circles) and the 6d <sup>3</sup>D<sub>2</sub> resonance (squares) as a function of the laser pulse energy.

## CHAPTER 3

### Collision-induced forbidden two-photon transitions to atomic Rydberg states of potassium.

P. Bicchi<sup>(a)</sup>, K. R. Mah, and F. W. Dalby.

Physics Department, University of British Columbia, Vancouver, British Columbia, Canada V6T 2A6.

## Abstract

We report the observation of the two-photon parity forbidden transitions  $4\ ^2S \rightarrow n\ ^2P$  of atomic potassium in resonantly enhanced multiphoton ionization spectra of a potassium vapor-argon gas mixture. The absorptions to the Rydberg  $\ ^2P$  levels were observed only for temperatures above  $190^\circ\text{C}$  where the atom densities are greater than  $8 \times 10^{13}\text{ cm}^{-3}$ . The forbidden absorptions to Rydberg final states are interpreted as a laser assisted single collision process. The characteristics of the forbidden spectra demonstrate that long range interactions between potassium atoms must be involved.

PACS numbers: 34.50.Rk, 32.80.Rm, 34.50.Gb

Laser-assisted or laser-induced collision processes have been the subject of a number of investigations in atomic and molecular physics in recent years <sup>1</sup>. In these processes, photon absorption occurs during a binary heavy-body collision. The final states of heavy-body collision products are usually inaccessible by the direct absorption of laser photons or by the heavy-body collision alone. It is the simultaneous interaction of the two collision reactants and the photon or photons that allows the final product states to be accessed.

Laser-assisted collisional absorptions involving Rydberg states have permitted forbidden atomic absorptions to occur in atomic sodium <sup>2</sup>. In this paper we report the observation of two-photon parity forbidden transitions to Rydberg states of atomic potassium,  $K^{**}$ , arising from the ground  $4s\ ^2S$  state of potassium in a potassium vapor-argon gas mixture<sup>3</sup>. We attribute the two-photon forbidden transitions to Rydberg  $np$  states to the absorption of two photons during a self- $l$ -mixing collision, that is,  $K^{**}$ - $K$  collision. These transitions were observed in resonantly-enhanced multiphoton ionization (RMPI) experiments performed under conditions such that there was near complete photoionization of the focal volume for the allowed transitions to  $nd$  states. RMPI is a well established technique that has been applied to the detection of many transitions in various atomic and molecular systems<sup>4-6</sup>.

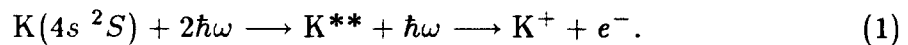
A schematic of the simple experimental apparatus is illustrated in Fig. 3.1. A cylindrical Pyrex cell of 25 mm diameter and 60 mm length contains a few Torr of argon and potassium at its saturated vapor pressure. The cells are constructed with two parallel 1 mm diameter tungsten wire electrodes separated by 10 mm. Several cells, all with the same construction geometry but with argon pressures varying from 1 to 10 Torr at room temperature were used. Potassium metal containing approximately 0.05% residual sodium impurity was distilled into the side finger of the cell. This reservoir of potassium is held at slightly lower temperatures than the body of the cell to prevent condensation on the cell windows. The cell is operated

inside an oven at fixed temperatures ranging from 150° C to 230° C corresponding to atomic densities of  $\sim 10^{13}$  to  $4 \times 10^{14}$  cm $^{-3}$ .

A Molelectron DL300 tunable dye laser pumped by a nitrogen laser produced light with a pulse duration of 5 ns, linewidth  $\sim 1.5$  cm $^{-1}$ , and at a repetition rate of 10 Hz. The light is focussed between the two electrodes along the axis to a minimum spot radius of  $\sim 40$   $\mu$ m. The dye laser covered wavelengths ranging from 5000 to 7300 Å and pulse energies ranged between 40 and 250  $\mu$ J. The corresponding power densities used in the experiments varied from 160 MW cm $^{-2}$  to 1 GW cm $^{-2}$  at the minimum beam waist. The laser intensity is attenuated, when needed, with calibrated neutral density filters and the light is made 100% linearly polarized with an external Glan prism. When circular polarization is required, the linearly polarized light is passed through a Soleil-Babinet compensator which has been adjusted to perform as a quarter-wave plate.

Resonant absorption is detected through the collection of the free electrons created by the laser-induced photoionization. The negative voltage applied to the cathode varied from 2 to 150 volts; thus, the performance of the ionization detection varied from ion chamber collection to amplification through gas multiplication. While the use of the low voltages resulted in recombination losses, they were necessary to demonstrate the appearance of the forbidden transitions in modest electric fields. After collection by the anode the electron current is passed through a preamplifier, monitored on an oscilloscope, processed by a PAR model 160 boxcar integrator, and displayed on a chart recorder.

The two-photon RMPI signals are due to the process



The excited Rydberg state, K $^{**}$  for the allowed two-photon resonances is either a  $^2S$  or a  $^2D$  state. For all conditions studied the series  $(n + 2) \ ^2S$  and  $n \ ^2D$  for

$4 \leq n \leq 32$  are observed. At temperatures above  $190^\circ$  C corresponding to vapor densities above  $8 \times 10^{13} \text{ cm}^{-3}$ , the two-photon transition, forbidden by the Laporte rule, to the  $n \ ^2P$  state are observed for  $13 \leq n \leq 20$ .

A portion of a spectrum taken with a cathode voltage of 10 volts and at a high temperature of  $232^\circ$  C is shown in Fig. 3.2. The spectrum is not normalized with laser intensity which is decreasing with decreasing wavelength in this figure. The forbidden  $\ ^2P$  resonances appear strongly at this temperature and exhibit the general feature that the relative intensity of the  $(n+2) \ ^2P$  signal to the  $n \ ^2D$  signal increases with increasing  $n$ . The resonant signals appear on a pedestal which has been established to be due to photoelectrons produced from scattered light impinging on potassium coatings on the electrodes or cell walls. When higher cathode voltages are used at the higher temperatures, the pedestal causes deterioration of signal to noise levels. However, the spectra obtained with low voltages suffer from nonlinearities in the ionization detection. This makes quantitative comparisons of the signals difficult. However, knowledge that the  $\ ^2S$  resonances are actually much weaker than the  $\ ^2D$  resonances from low density ( $\sim 10^{11} \text{ cm}^{-3}$ ) two-photon RMPI experiments<sup>7</sup> enables us to make some correction for the nonlinearities. We estimate that the forbidden signals are actually an order of magnitude weaker than they appear in our spectra taken with low voltages.

We attribute the forbidden absorptions to the laser-assisted collision process



where the photon energy,  $\hbar\omega$  is equal to one-half the  $n \ ^2P - 4 \ ^2S$  energy difference. The process is regarded as one in which a self- $l$ -mixing collision occurs in the presence of the exciting radiation. The self- $l$ -mixing collisions of Rydberg atoms have enormous interaction cross sections of the order of the Rydberg geometric cross section<sup>8</sup> or possibly larger. Cross sections several orders of magnitude larger

than the geometric cross sections have been demonstrated for resonant collisions involving Rydberg K atoms<sup>9</sup>. After the long range collision the final state of the Rydberg atom has acquired various  $l$  character. The observed forbidden two-photon transitions occur between the ground  $4s\ ^2S$  state and the  $d$  component of the final mixed state. Although one of the collision reactants is described as being a  $^2P$  Rydberg state, clearly the two-photon excitation to a  $^2P$  state has not occurred before the collision takes place. The process must be interpreted as the absorption and collision processes being simultaneous. Similar effects been observed recently in sodium<sup>2</sup> and magnesium<sup>10</sup>.

The process described by reaction (2) must have a quadratic dependence on the atom density,  $N$ . If the  $^2P$  excitations are the result of electric quadrupole processes or Stark mixing of  $n\ ^2P$  states with nearby levels, the forbidden RMPI signals would exhibit a linear dependence on  $N$ . Because the range of atom densities over which the  $^2P$  resonances are observed is relatively small (less than a factor of 10), the  $N$  dependence cannot be measured reliably to rule out electric quadrupole processes or Stark mixing. However, as we will discuss later, we have found that there are features in the spectra that support reaction (2). In addition, we have investigated the possibility that electric quadrupole processes and Stark mixing are responsible for the forbidden transitions and find no reason to consider them under our experimental conditions.

The  $^2P$  signals are estimated to be one or two orders of magnitude smaller than the allowed signals. Since the strength of electric dipole transitions are more than  $10^5$  times larger than those of quadrupole transitions, the observed ratio implies that the quadrupole processes do not contribute significantly to the production of the forbidden signals.

Significant Stark mixing could be possible because the wire electrodes apply a fairly uniform dc electric field to the interaction region. Field-induced RMPI signals in modest (12 – 120 V/cm) dc electric fields have been observed in potassium

by Teraoka et al.<sup>7</sup> To determine whether Stark mixing is significant the spectra were studied as the applied field was varied. When the fields in the interaction region were varied from 2 V/cm to 120 V/cm (the maximum field before gas breakdown), we did not measure an appreciable change in the size of the  $^2P$  signals. This comparison was corrected for the effect varying the cathode voltage has on the performance of the ionization detection. If Stark mixing was responsible, the forbidden signals should exhibit a quadratic dependence on the applied field<sup>11</sup>. Furthermore, Stark mixing should be independent of  $N$  and would also be observed at the lower temperatures of our study. We emphasize that the  $^2P$  signals are observed only at the higher densities while Teraoka et al. and Wheatley et al.<sup>6</sup> observed the field-induced RMPI signals at densities lower than ours. While the work by Teraoka et al. was done in modest fields, the Stark mixing for the lowest fields (12 V/cm) were observed for large values of the principal quantum number ( $n > 22$ ). Wheatley et al. observed Stark mixing in much larger fields (700 V/cm) than we used. From the above considerations we conclude that Stark mixing by the applied electric field is not important here.

Stark mixing by the microfields of the laser-induced plasma in the focal region was also investigated. We calculate that the required ion density to produce sufficient mean electric fields to give the observed signal strengths would require 1 to 10% ionization of the focal volume. That ionization yield is produced only for the  $^2D$  resonances; therefore, sufficient ion densities are not achieved for the  $^2P$  resonances. In addition, we cannot determine how such a plasma could form off resonance to perturb the nearby  $^2D$  levels.

For the allowed transitions we observed, as expected, the appearance of both the  $^2S$  and  $^2D$  resonances with the incident light linearly polarized and the absence of the  $^2S$  resonances when circularly polarized light is used. With circularly polarized light the signals of the  $^2D$  resonances increased and the signals of the

${}^2P$  resonances increased by the same relative amount. This observation is consistent with the  $l$ -mixed final state of the forbidden resonance having a predominantly  $d$ -character.

The forbidden signals decrease with decreasing  $n$  and vanished for  $n \leq 13$  over the range of atom densities studied. However the signal measured at the 14  ${}^2P$  resonance was found to be larger than the other  ${}^2P$  signals. This is due to the frequency coincidence, within our laser bandwidth, of the two-photon forbidden transition ( $\bar{\nu} = 17\,141.4\text{ cm}^{-1}$ ) with the hybrid resonance<sup>12,13</sup>  $4\,{}^2P_{3/2} \rightarrow 5\,{}^2D_{3/2,5/2}$  ( $\bar{\nu} = 17\,142.9\text{ cm}^{-1}$ ). The hybrid resonance signals correspond to the excitation of a  $\text{K}_2$  or  $\text{NaK}$  molecule from the ground state to a repulsive excited state which rapidly dissociates to produce an excited  ${}^2P$  atom. The absorption of a resonant photon takes the atom from the excited  ${}^2P$  state to a  $n\,{}^2D$  state which is ionized by the absorption of another laser photon. Additional hybrid resonances of  $\text{K}$ ,  $4\,{}^2P_{3/2} \rightarrow n\,{}^2D_{3/2,5/2}$ , were observed for  $n = 6$  and  $7$ . Also observed were hybrid resonances in  $\text{Na}$  originating from the excited  $3\,{}^2P$  levels. The  $\text{Na}$  hybrid resonances were  $3\,{}^2P_{3/2} \rightarrow 4\,{}^2D_{3/2,5/2}$  and  $3\,{}^2P_{3/2} \rightarrow 4\,{}^2D_{3/2}$ . The hybrid resonance signals are quite temperature dependent since sufficient atom densities are required such that the number of molecules formed becomes significant. We remark that the observation of the hybrid resonances only for  $T \geq 190^\circ\text{C}$  appears correlated to the appearance of the forbidden signals for the same temperatures. This correlation provides support to the suggestion that the forbidden signals have a quadratic dependence on the atom density.

Because of the long-range nature of the collisions, the duration of the collisions are correspondingly long; hence, narrow absorption linewidths are a feature of reaction (2). The allowed  ${}^2S$  and  ${}^2D$  signals have linewidths of  $2\text{ cm}^{-1}$  which is greater than the laser linewidth because of the high light intensities used. Within the experimental uncertainty the linewidths of the  ${}^2P$  signals are found to be the

same as those for the  $^2S$  and  $^2D$  signals. Our observations indicate that the broadening of the  $^2P$  lines is less than our laser linewidth and appears consistent with reaction (2). Noticeable broadening would be expected if the signals were induced by short-range collisions.

The results of our investigations support the interpretation that the two-photon forbidden  $^2P$  signals are the result of long-range self- $l$ -mixing collisions in the presence of resonance radiation. We note that while we describe the interaction as a laser-assisted single collision process, other explanations have been given for two-photon forbidden excitations. In Mg vapor at considerably higher atom densities, the excitations were interpreted as arising from the two-photon excitation of a quasi-molecule, a Rydberg excimer  $Mg_2$  which is formed by collisions due to long-range dispersion and exchange forces<sup>10</sup>. While the exact mechanism responsible for the observations has not been established, we have demonstrated that long-range interactions must be involved.

We thank Professor A. Kopystynska and Professor M. H. L. Pryce for the many useful discussions and helpful comments. We also thank Professor R. Bernheim for kindly reading the manuscript. We gratefully acknowledge the assistance in data acquisition by C. Araujo. One of us (P. B.) was partially supported by a NATO Senior Fellowship grant. This work was supported by the Natural Sciences and Engineering Research Council of Canada.

<sup>(a)</sup>Permanent address: Istituto di Fisica, Università di Siena, Via Banchi di Sotto, 55/57, 53100 Siena, Italy.

<sup>1</sup>See, for example, *Collisions and Half Collisions with Lasers*, edited by N. K. Rahman and C. Guidotti (Harwood-Academic, Chur, Switzerland, 1984); A. Kopystynska and L. Moi, Phys. Rep. **92**, 135 (1982).

<sup>2</sup>C. E. Burkhardt, M. Ciocca, W. P. Garver, J. J. Leventhal, and J. D. Kelley, Phys. Rev. Lett. **57**, 1562 (1986).

<sup>3</sup>P. Bicchi, K. R. Mah, and F. W. Dalby, in *Book of Abstracts of the Second European Conference on Atomic and Molecular Physics, Amsterdam, 1985* edited by A. E. de Vries and M. J. van der Wiel, p. 4.

<sup>4</sup>G. Petty, C. Tai, and F. W. Dalby, Phys. Rev. Lett. **34**, 1207 (1975).

<sup>5</sup>P. M. Johnson, M. R. Berman, and D. Zakheim, J. Chem. Phys. **62**, 2500 (1975).

<sup>6</sup>S. E. Wheatley, P. Agostini, S. N. Dixit, and M. D. Levenson, Physica Scripta **18**, 177 (1978).

<sup>7</sup>Y. Teraoka, Y. Sato, and J. Murakami, Phys. Rev. A **32**, 3742 (1985).

<sup>8</sup>M. Hugon, F. Gounand, and P. R. Fournier, J. Phys. B **13**, L109 (1980).

<sup>9</sup>R. C. Stoneman, M. D. Adams, and T. F. Gallagher, Phys. Rev. Lett. **58**, 1324 (1987).

<sup>10</sup>J. T. Zhang, H. T. Zhou, J. Yang, Q. R. Li, and K. T. Lu, in *Abstracts of the Tenth International Conference on Atomic Physics, Tokyo, 1986* edited by H. Narumi and I. Shimamura, p. 212.

<sup>11</sup>E. U. Condon and G. H. Shortley, *The Theory of Atomic Spectra* (Cambridge University Press, London, 1970).

<sup>12</sup>N. M. Shen and S. M. Curry, Opt. Commun. **20**, 392 (1977).

<sup>13</sup>H. Kato and C. Noda, J. Chem. Phys. **73**, 4940 (1980).

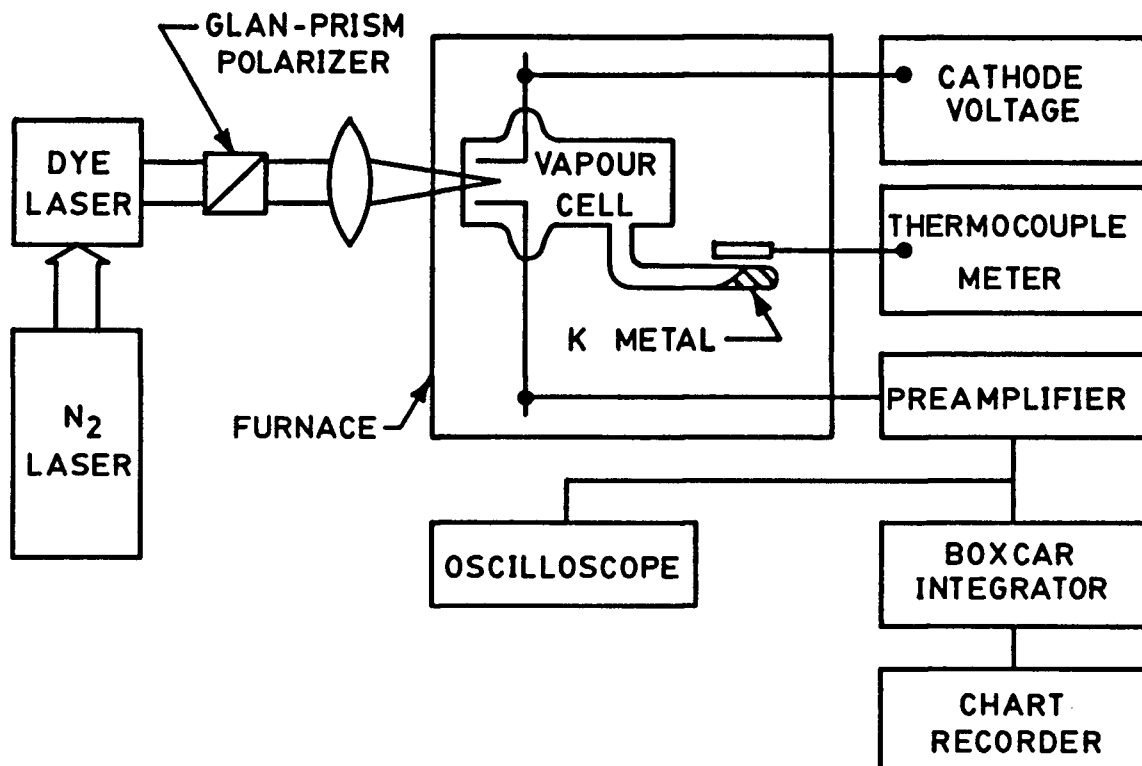


Fig. 3.1 Schematic diagram of the photoionization experiment. When circularly polarized light is required, a Soleil-Babinet compensator (not shown) is used after the Glan-prism polarizer.

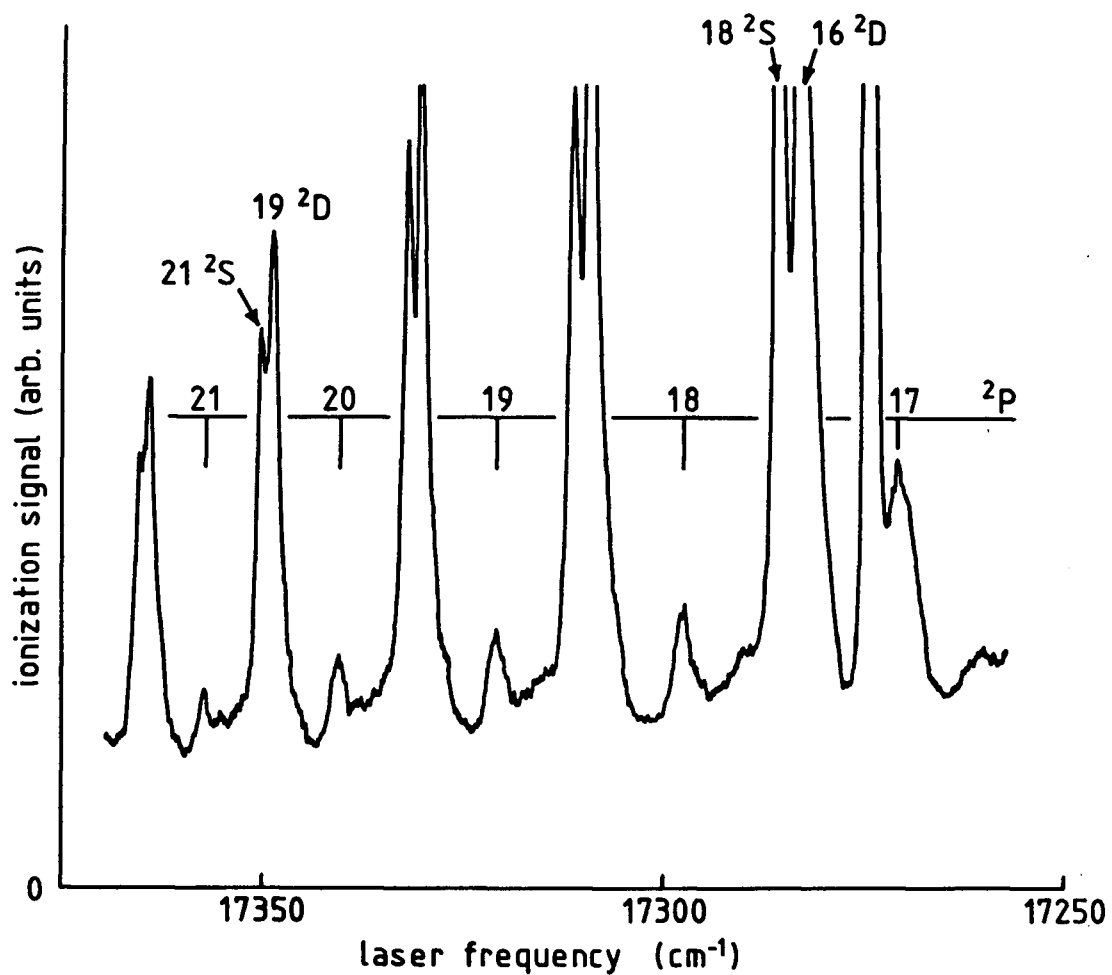


Fig. 3.2 Portion of a potassium resonant multiphoton ionization spectra taken at  $T=232^{\circ}\text{C}$  and with a collection voltage of 10 volts. The laser power density was  $800\text{ MW cm}^{-2}$ . The strong single line signal near  $17\,275\text{ cm}^{-1}$  is due to the sodium impurity.

## CHAPTER 4

### Conclusions

The most significant conclusion of Chapter 2 is that the saturation of the ionization step is the primary obstacle to the measurement of photoionization cross sections with RMPI techniques. The presence of saturation effects was not immediately obvious until the dynamics of the RMPI process were examined. Saturation effects can easily be overlooked when ionization yields are considered alone. With approximately  $10^{-7}$  of the atoms in the focal volume ionized, saturation of the RMPI appears unlikely. In addition, a saturated ionization process would normally be expected to have an ion yield that exhibits little or no dependence on the light polarization and intensity. Careful analysis of the data and the dynamics of the RMPI resulted in the conclusion that the ionization step was completely saturated and the measured polarization dependences reflected the polarization dependence of the ionization step. After an examination of the transition rates, the treatment of the RMPI as a two step process was introduced. Two types of saturation within the RMPI process could be defined for this simple model, and the saturation of the ionization step in the experiment was recognized. From the study of the two step model, the general observation can be made: complete photoionization of the resonant level will be difficult to avoid when the magnitude of the coupling of the ground state to the resonant level is much less than the coupling of the resonant level to the continuum. Reduction of the laser irradiances to prevent the saturation

of the ionization step would result in ion yields too small to measure especially for RMPI experiments with resonant excitation steps requiring more than two photons.

The investigations have demonstrated that nonlinear or perturbation processes of RMPI can significantly affect polarization measurements. In particular, the RMPI absorption profile of the  $6d\ ^1D_2$  resonance was observed to vary with the polarization of the light. A thorough investigation of this feature should be performed. Correlations to the AC Stark effect, which is suspected to be responsible, should also be attempted. A laser with a narrower bandwidth, simpler frequency mode structure, and cleaner spatial transverse mode structure would be strongly recommended for studies of the absorption profile. These improvements would assist the making of applicable models for the inhomogeneous line broadening by the AC Stark shifts.

Another promising aspect that was encountered and only briefly mentioned in Chapter 2 was the effect that increasing the mercury pressures had on the spectra. At the pressures used in the polarization measurements, some evidence of cooperative effects between mercury atoms was observed. In preliminary measurements at mercury pressures up to  $\sim 200$  Torr, the RMPI spectra of the  $3 + 1$  ionizations on P and F resonances displayed extreme line broadening and shifts (well over ten times the laser bandwidth) and new broad structures. These effects are due to the cooperative effects leading to the third harmonic generation of coherent VUV light. Reabsorption of the VUV light<sup>1</sup> is partly responsible for the broadening of the ionization signals. Since there has been recent studies of the interferences between the three-photon excitation and the excitation of the coherently generated field<sup>2</sup> at lower pressures, studies of the RMPI spectra at higher pressures should be continued. Identifications of the structures and the underlying mechanisms of the high pressure spectra will be quite challenging. Direct observations of the third harmonic will probably be necessary, but difficulties may be encountered by the strong reabsorption of the VUV emission at these mercury densities. In addition,

further investigations of the  $4 + 1$  ionization spectra on the  $6d\ ^1,^3D_2$  and  $7s\ ^1S_0$  resonances at the high pressures could be performed and possibly related to the work on four-photon resonant third harmonic generation in mercury by A. V. Smith.<sup>3</sup>

In the investigations of Chapter 3, density dependent forbidden two-photon resonances have had their excitation process identified as a photon-assisted collision. The observation of photon-assisted collisions with narrow absorption linewidths is a relatively new phenomena, and we expect theoretical investigations will soon provide results for experimental comparisons.

Some aspects of the work of Chapter 3 are incomplete, but further investigations on them may be difficult to carry out even with an upgrade of the experimental system. A demonstration of a quadratic atom density dependence for the forbidden  $^2P$  signals would provide very strong additional evidence for the explanation that long range interactions are responsible. As mentioned earlier the densities at which the  $^2P$  signals are first observable cannot be increased even by one order of magnitude without the rapid deterioration of the glass cell. While alkali resistant glasses should be tried, there are difficulties in the ionization detection at the higher atom densities. The present technique of simple ion chamber collection with no gas multiplication is not very sensitive nor efficient because of the need to use low collection fields to prevent Stark effects. Better sensitivity could be obtained by the use of ion or electron multipliers; however, the high vacuum requirements of these instruments prevents their use at the suggested high densities.

Lower laser irradiances would be desirable to reduce the detector saturation which occurs for the allowed two-photon resonances. Proper comparisons of the forbidden signals to the allowed signals could then be made. Unfortunately the limited dynamic range of the present detection system and the high noise levels of the pedestal, seriously limit the reduction of the laser irradiances.

The following discussion is on two observations that should be considered for future work. Argon buffer gas was used in the present investigations in which gas

multiplication techniques were used to increase the detection sensitivity. After the forbidden signals were observed, the need to eliminate large external electric fields made simple ion collection necessary, but the same sealed cells containing argon were used. Argon is not considered a significant perturber for the mixing of angular momentum states (self- $l$ -mixing is dominant<sup>4</sup>). Since argon probably plays no role in the collision interactions and is not necessary for the ion detection, its use should be discontinued for future investigations.

The other observation that deserves to be explored may be related to the pedestal in the spectrum (see Fig. 3.2). As the Rydberg spectra was studied up to the two-photon ionization limit (where the third photon is no longer required to ionize), a sharp increase in the ionization signal was not observed at the ionization limit even for the moderate densities. The discontinuity may have been obscured by the pedestal. In order to do studies near the ionization limit, a serious effort must be given to the normalization of the ionization signals to the laser power. Because near the ionization limit, the power output curves of the dye laser drop rapidly and the processes are nonlinear with laser power, the signals fall extremely fast and relative comparisons become difficult. Investigations near the ionization limit may improve the understanding of the perturbations<sup>5</sup> present in the experiments and the effects of the pedestal.

## References and notes

<sup>1</sup>in fact, sharp peaks, observed in the shoulders of the broadened lines, were found to correspond to atomic absorption lines.

<sup>2</sup>W. R. Garrett, W. R. Ferrell, M. G. Payne, and J. C. Miller, Phys. Rev A **34**, 1165 (1986).

<sup>3</sup>A. V. Smith, Opt. Lett. **10**, 341 (1985).

<sup>4</sup>M. Hugon, F. Gounand, P. R. Fournier and J. Berlande, J. Phys. B **12**, 2707 (1979).

<sup>5</sup>for examples of perturbations near the ionization limit see Ref. 7 of Chapter 3.